OPEN

LncRNA *ZFAS1* as a SERCA2a Inhibitor to Cause Intracellular Ca²⁺ Overload and Contractile Dysfunction in a Mouse Model of Myocardial Infarction

Ying Zhang,* Lei Jiao,* Lihua Sun, Yanru Li, Yuqiu Gao, Chaoqian Xu, Yingchun Shao, Mengmeng Li, Chunyan Li, Yanjie Lu, Zhenwei Pan, Lina Xuan, Yiyuan Zhang, Qingqi Li, Rui Yang, Yuting Zhuang, Yong Zhang, Baofeng Yang

Rationale: Ca²⁺ homeostasis—a critical determinant of cardiac contractile function—is critically regulated by SERCA2a (sarcoplasmic reticulum Ca²⁺-ATPase 2a). Our previous study has identified *ZFAS1* as a new lncRNA biomarker of acute myocardial infarction (MI).

Objective: To evaluate the effects of *ZFAS1* on SERCA2a and the associated Ca²⁺ homeostasis and cardiac contractile function in the setting of MI.

Methods and Results: *ZFAS1* expression was robustly increased in cytoplasm and sarcoplasmic reticulum in a mouse model of MI and a cellular model of hypoxia. Knockdown of endogenous *ZFAS1* by virus-mediated silencing shRNA partially abrogated the ischemia-induced contractile dysfunction. Overexpression of *ZFAS1* in otherwise normal mice created similar impairment of cardiac function as that observed in MI mice. Moreover, at the cellular level, *ZFAS1* overexpression weakened the contractility of cardiac muscles. At the subcellular level, *ZFAS1* deleteriously altered the Ca²⁺ transient leading to intracellular Ca²⁺ overload in cardiomyocytes. At the molecular level, *ZFAS1* was found to directly bind SERCA2a protein and to limit its activity, as well as to repress its expression. The effects of *ZFAS1* were readily reversible on knockdown of this lncRNA. Notably, a sequence domain of *ZFAS1* gene that is conserved across species mimicked the effects of the full-length *ZFAS1*. Mutation of this domain or application of an antisense fragment to this conserved region efficiently canceled out the deleterious actions of *ZFAS1*. *ZFAS1* had no significant effects on other Ca²⁺-handling regulatory proteins.

Conclusions: *ZFAS1* is an endogenous SERCA2a inhibitor, acting by binding to SERCA2a protein to limit its intracellular level and inhibit its activity, and a contributor to the impairment of cardiac contractile function in MI. Therefore, anti-*ZFAS1* might be considered as a new therapeutic strategy for preserving SERCA2a activity and cardiac function under pathological conditions of the heart. (*Circ Res*. 2018;122:1354-1368. DOI: 10.1161/CIRCRESAHA.117.312117.)

Key Words: calcium ■ myocardial infarction ■ RNA, long noncoding ■ sarcoplasmic reticulum calcium-transporting ATPases

---

The heart beats rhythmically to drive blood circulating throughout the body, and each single heart beat begins with the initial phase with Ca²⁺ influx into cells and Ca²⁺ release from sarcoplasmic reticulum (SR) through RyR2 (ryanodine receptor 2) to trigger contraction of cardiac muscles, followed by the second phase

with Ca²⁺ reuptake or load to SR to render relaxation of cardiac muscles. Thus, intracellular Ca²⁺ homeostasis is critical to cardiac

---

Novelty and Significance

What Is Known?

- Cardiac function depends on properly controlled concentration of calcium within the myocardium, and excess calcium (or calcium overload) in cardiac muscles is deemed to cause severe impairment of cardiac function.
- SERCA2a (sarcoplasmic reticulum Ca^{2+}-ATPase 2a) is the major regulator of calcium concentration in cardiac muscles, and reduction of SERCA2a level or dysfunction of this protein can result in calcium overload and cardiac dysfunction.
- The levels and activity of SERCA2a are tightly regulated in cardiac muscles; however, the mechanisms regulating SERCA2 remain unclear.

What New Information Does This Article Contribute?

- ZFAS1—a member of long nonprotein-coding RNAs—is increased in the mouse myocardium after infarction, and artificial mitigation of this increase restores the impaired contractile dysfunction after myocardial infarction.
- ZFAS1 acts as a natural inhibitor of SERCA2a. It reduces the level and function of SERCA2a, causing calcium overload and cardiac dysfunction through direct RNA–protein interactions.

- A specific sequence motif of ZFAS1 was identified as the functional domain responsible for the anti-SERCA2a action of the full-length *ZFAS1*.

An important mechanism underlying myocardial dysfunction after infarction is abnormal calcium accumulation, or calcium overload muscles, which is often the consequence of decreased level or impaired function of SERCA2a—a key molecule regulating calcium homeostasis. We identified a lncRNA, ZFAS1, as a natural inhibitor of SERCA2a in cardiac muscles. Specifically, we found that levels of ZFAS1 were abnormally increased after myocardial infarction, and this increase was associated with impaired cardiac function. Artificial suppression of ZFAS1 abrogated these anomalies. At the subcellular level, ZFAS1 caused calcium overload, and at the molecular level, ZFAS1 decreased the level and function of SERCA2a by direct binding to this protein. These findings provide insights into the role of lncRNA in regulating SERCA2a and the associated cardiac function. Inhibition of ZFAS1 could be a viable therapy for ameliorating cardiac dysfunction associated with calcium overload.

Nonstandard Abbreviations and Acronymse	
AsZFAS1-FD	antisense fragment corresponding to the functional domain of *ZFAS1*
CUPID2	Calcium Upregulation by Percutaneous Administration of Gene Therapy in Patients With Cardiac Disease
EF	ejection fraction
LV	left ventricular
MI	myocardial infarction
NFATc2	nuclear factor of activated T cells C2
NFATc3	nuclear factor of activated T cells C3
NMCMs	neonatal mouse cardiomyocytes
PLN	phospholamban
RyR2	ryanodine receptor 2
SERCA2a	sarcoplasmic reticulum Ca^{2+}-ATPase 2a
shZFAS1-V	adeno-associated virus 9 vector carrying a ZFAS1-shRNA fragment
SR	sarcoplasmic reticulum
SS	sarcomere shortening
ZFAS1-FD	functional domain of *ZFAS1*
ZFAS1-V	adeno-associated virus 9 vector carrying the *ZFAS1* gene

contractile function and is delicately regulated by a large body of proteins in a highly coordinated manner.[1,2] Among these regulatory proteins, SERCA2a (SR Ca^{2+}-ATPase 2a) is the key protein that governs the normal intracellular Ca^{2+} handling process and thereby cardiac contractile function by mediating Ca^{2+} reuptake into SR in cardiac muscles.[3] SERCA2a activity is susceptible to various cellular environmental cues and is under the tight regulation by an array of factors. SERCA2a function can be impaired as a result of either expression deregulation (mostly downregulation) or activity depression leading to deficiency of Ca^{2+} reuptake back to SR

leading to intracellular Ca^{2+} overload. The consequence of this is manifested by impairment of cardiac contractile function and by cardiomyocyte apoptosis as well.[4,5] Indeed, SERCA2a dysfunction has been associated with a wide spectrum of cardiovascular diseases, such as myocardial infarction (MI), cardiac hypertrophy, arrhythmias, ischemia/reperfusion, and heart failure especially.[6–10] Both basic scientists and clinical practitioners have shown their enthusiasm on the potential of SERCA2a overexpression/replacement as a therapeutic strategy.[11–13] However, a recent randomized, double-blind, placebo-controlled clinical trial named CUPID2 (Calcium Upregulation by Percutaneous Administration of Gene Therapy in Patients With Cardiac Disease) presented negative results on the benefit of SERCA2a overexpression in patients with advanced heart failure with the lack of improvement of reduced ejection fraction (EF).[14] The authors proposed the inadequate dose of SERCA2a as one of the explanations for the lack of benefit of SERCA2a in their study. Clearly, the benefits of SERCA2a replacement have not been well established in the clinical settings, and our understanding of the precise mechanisms for the pathological expression downregulation and functional depression of SERCA2a and the multilayer complex regulatory network for Ca^{2+} handling is still far from being complete. This constitutes an obstacle for the potential clinical applications of SERCA2a replacement to the treatment of heart disease.

MI is the worst threat to human lives, and it affects an increasing number of individuals worldwide. This is because MI is not only the main cause of sudden cardiac death but also the primary process leading to heart failure.[15–17] MI is a metabolic catastrophe characterized by contractile dysfunction, arrhythmia, and cell death because of reduced supply of O_2 and nutrients to the myocardium. Hypoxia—a condition of insufficient O_2 supply to support metabolism—is a frequently encountered problem of the cellular microenvironment and a major factor in the pathology of MI.[18] The contractile dysfunction occurring in MI or hypoxia is primarily caused by

impairment of intracellular Ca^{2+} homeostasis because of the chaos of Ca^{2+} handling.[19–21] SERCA2a dysfunction as a causal factor for intracellular Ca^{2+} overload and cardiac contractile dysfunction in the setting of MI has been well documented by many research groups.[22–24] Yet, how SERCA2a expression and function are regulated during MI remained poorly understood.

Human genome sequencing and GENCODE (human genome encyclopedia of DNA elements) project have revealed that only ≈2% of the human genome can be translated into proteins and the rest of it is primarily transcribed into ncRNAs.[25,26] Recently, several lncRNAs have been reported to be involved in heart disease.[27–35] In addition, lncRNAs are also emerging as biomarkers for cardiovascular diseases.[29,35] In our previous study, we identified *ZFAS1*—an antisense lncRNA to the 5′ end of the protein-coding gene *ZNFX1*—as an independent predictor of acute MI.[29] Intriguingly, *ZFAS1* level was found to be markedly decreased in the bloodstream but elevated in the myocardium. We have, therefore, proposed that in addition to its potential as a biomarker of MI, *ZFAS1* might also contribute to the development of MI.[29]

This thought prompted us to carry out the present study to exploit the role of *ZFAS1* in the pathological process associated with MI and to decipher the underlying molecular and signaling mechanisms. Specifically, we investigated the effects of *ZFAS1* on cardiac contractile function and intracellular Ca^{2+} handling with both gain- and loss-of-function approaches in a mouse model of MI and a cellular model of hypoxia. Our experimental results indicate that *ZFAS1* is a detrimental factor to the heart in the setting of MI, and knockdown of this lncRNA is able to mitigate the ischemic contractile dysfunction.

Methods

The data that support the findings of this study are available from the corresponding author on reasonable request.

Human Samples

Human cardiac preparations used in this study were collected from the Tissue bank of the Heilongjiang Academy of Medical Sciences (Harbin, China). The use of human cardiac tissues for the present study was approved from the Ethics Committee of the Harbin Medical University (No. HMUIRB20170034). Our study protocols complied with the guidelines that govern the use of human tissues outlined in the Declaration of Helsinki.

Mouse Model of MI

C57BL/6 mice ranging from 8 to 10 weeks in age and weighing between 22 and 25 g each were used for animal studies, and pregnant C57BL/6 mice were used for neonatal myocyte isolation (Animal Experimental Ethical Inspection Protocol No. HMUIRB20170034). Use of animals was approved by the Ethic Committees of Harbin Medical University and conformed to the Guide for the Care and Use of Laboratory Animals published by the US National Institutes of Health (Publication No. 85-23, revised 1996).

Data Analysis

Data are expressed as mean±SEM and were analyzed with SPSS 13.0 software. Statistical comparisons among multiple groups were performed using ANOVA followed by Dunnett test. Student *t* test was performed for comparisons between 2 groups. A 2-tailed *P*<0.05 was taken to indicate a statistically significant difference. Nonlinear least square curve fitting of raw data points was performed with GraphPad Prism.

Detailed descriptions on the materials and methods used in this study are provided in the Online Data Supplement.

Results

Upregulation of *ZFAS1* Expression in Ischemic Hearts and Hypoxic Cardiomyocytes

We have demonstrated in our recently published study that *ZFAS1* expression is markedly elevated in the myocardium of mice with acute MI (from 1 to 24 hours post-MI).[29] Here, we verified this result in MI mice: compared with the sham group, the expression level of *ZFAS1* was increased by 1.8-fold in mouse myocardium 12 hours after MI (Figure 1A, left). Similar increase in *ZFAS1* level was also observed in human myocardium from patients with MI (Figure 1A, right).
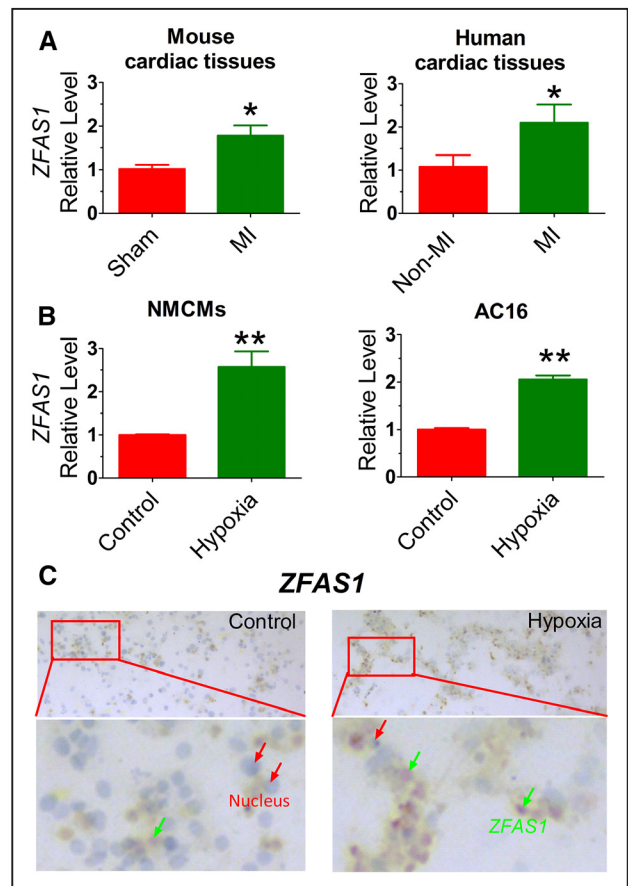
Figure 1. Upregulation of *ZFAS1* expression in ischemic heart and in hypoxic cardiomyocytes. A, Elevation of cardiac *ZFAS1* level in the peri-infarct areas of a mouse model of myocardial infarction (MI; **left**) and of myocardium from patients with MI (**right**). Mouse MI was created by ligation of the left descending coronary artery, and the measurements were conducted 12 h after MI. *ZFAS1* levels were determined by real-time polymerase chain reaction (same below). **P*<0.05, MI mice vs Sham mice (n=6) or patients with MI vs without MI (n=3). **B,** Increase in *ZFAS1* expression in cultured neonatal mouse cardiomyocytes (NMCMs; **left**) and in AC16 cells (adult human ventricular cardiomyocyte cell line; **right**) after hypoxia treatment for 12 h, relative to the cells kept under normoxic conditions. ***P*<0.01, hypoxia vs control; n=≈4–6. Above data are presented as mean±SEM. **C,** Representative images of In Situ Hybridization (ISH) in NMCMs showing an increase in *ZFAS1* expression after hypoxia treatment for 12 h. Note that *ZFAS1* was distributed evenly in both cytosol and nucleus. Red arrows pointing to the nucleus stained in light blue and green ones pointing to *ZFAS1* stained in brown. Images are presented with a magnification of ×100 for the (**top**) and ×500 for the (**bottom**). Similar results were consistently observed in another 3 batches of cells.

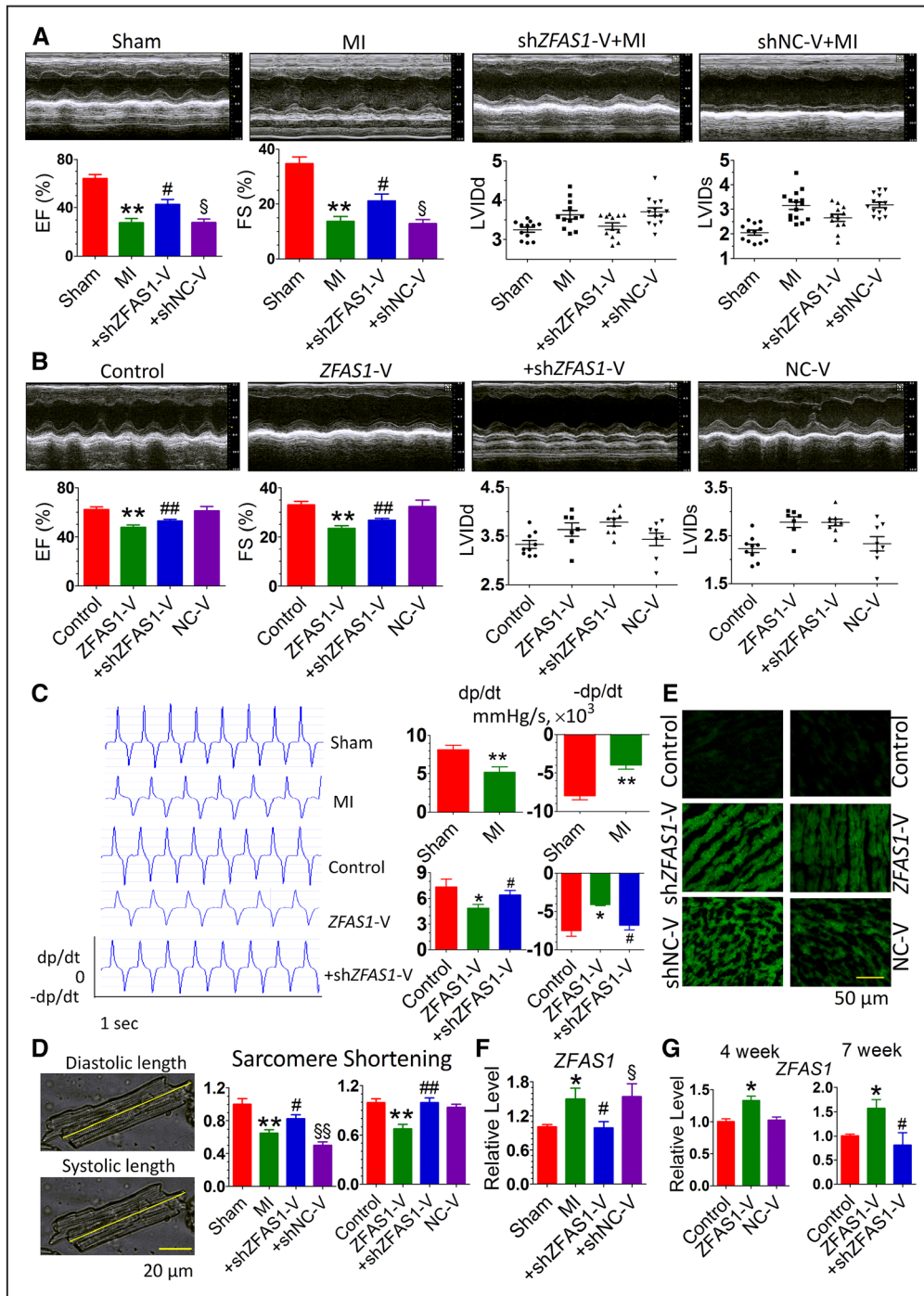**Figure 2. Impairment of cardiac contractile function by *ZFAS1* in myocardial infarction (MI) mice. A**, Amelioration of impairment of contractile function by *ZFAS1* overexpression produced by the recombinant adeno-associated virus (serotype 9; AAV9) vector carrying the shRNA (sh*ZFAS1*-V) to knock down endogenous *ZFAS1* in MI mice. The viral constructs were intravenously injected into mice. Note that sh*ZFAS1*-V abrogated the ischemia-induced decreases in ejection fraction (EF) and fractional shortening (FS), and enlargement of left ventricular internal dimension at end diastole (LVIDd) and left ventricular internal dimension at systole (LVIDs). shNC-V: the negative control shRNA engineered into the AAV9 vector. **P<0.01 vs Sham, #P<0.05 vs MI, §P<0.05 vs sh*ZFAS1*-V; n=≈12–18. **B**, Impairment of contractile function induced by *ZFAS1* overexpression generated by AAV9 vector carrying the full-length *ZFAS1* gene (AAV9 vector carrying the ZFAS1 gene [*ZFAS1*-V]) in healthy mice. Note that *ZFAS1*-V significantly decreased EF and FS, and increased LVIDd and LVIDs, similar to those seen in MI mice, and these effects were essentially reversed by coinjection of sh*ZFAS1*-V. NC-V: the empty AAV9 vector as a negative control for *ZFAS1*-V. **P<0.01 vs control or NC-V, ##P<0.01 vs *ZFAS1*-V; n=≈7–10. **C**, Decreased maximum rate of rise of left ventricular pressure during contraction (+dp/dt$_{max}$) and the maximum rate of drop of left ventricular pressure during relaxation (−dp/dt$_{max}$) in MI mice. **P<0.01 vs Sham. *ZFAS1* overexpressed by *ZFAS1*-V delivery showing reduced ±dp/dt$_{max}$. *P<0.05 vs control, #P<0.05 vs *ZFAS1*-V; n=3. **D**, Raw traces (**left**) showing the changes of sarcomere shortening (SS) as an index of contractility of cardiac muscles isolated from MI hearts, and mean values of SS in the presence of sh*ZFAS1*-V (**middle**) or *ZFAS1*-V (**right**). **P<0.01 vs Sham or control or NC-V, #P<0.05 vs MI, ##P<0.01 vs *ZFAS1*-V, §§P<0.01 vs sh*ZFAS1*-V; n=≈20–43. **E**, Representative cardiac sections showing the successful delivery of sh*ZFAS1*-V and *ZFAS1*-V into mouse myocardium in vivo the significant presence (*Continued*)

Hypoxia is a crucial event in the setting of MI, and it alone can cause many of the detrimental alterations of ischemic myocardium.[36,37] We thought that hypoxia might be sufficient to cause upregulation of *ZFAS1* as MI did. Our experiments conducted with cultured neonatal mouse cardiomyocytes (NMCMs) indeed generated the data showing a significant increase in *ZFAS1* level after exposure to hypoxic environment for 12 hours (2.6-fold up; *P*<0.01; Figure 1B, left). Qualitatively the same results were reproduced in adult human ventricular cardiomyocyte cell line AC16 cells cultured under hypoxic condition (*ZFAS1* upregulated by 2-fold; *P*<0.01; Figure 1B, right), relative to that in cells kept under normoxic condition.

Moreover, in situ hybridization in NMCMs showed markedly increased abundance of *ZFAS1*, as indicated by enhanced staining in brown, after exposure to hypoxic conditions, relative to the normoxic conditions (Figure 1C). Also noted was that *ZFAS1* is distributed in both cytoplasm and nucleus.

Impairment of Cardiac Contractile Function by *ZFAS1* in MI Mice

A question we asked was whether the upregulation of *ZFAS1* in MI is a contributor to ischemic cardiac injuries or is merely a bystander or a consequence of MI. To clarify this issue, we investigated the effects of *ZFAS1* on cardiac function in vivo using echocardiography. We first used a loss-of-function strategy with adeno-associated virus serotype 9 vector carrying a *ZFAS1*-shRNA fragment (sh*ZFAS1*-V) and investigated whether *ZFAS1* knockdown could alter cardiac function. Adeno-associated virus serotype 9 was chosen because it is one of the most promising gene transfer tools for gene therapy, and it has been demonstrated to have impressively high infection efficiency and safety profile in cardiac tissue.[38] As illustrated in Figure 2A, both EF and FS (fractional shortening) were substantially lower in the MI mice, compared with the sham-operated control counterparts. Moreover, left ventricular (LV) internal dimension at end diastole and LV internal dimension at systole were both enlarged. These changes indicated severe cardiac dysfunction in our MI model. Strikingly, in the MI mice that had received sh*ZFAS1*-V for 4 weeks, the abovementioned parameters of cardiac function were all improved with EF and fractional shortening nearly recovered back to normal levels (Figure 2A). In addition, there was a decrease in LV anterior wall thickness and dilatation, as reflected by the diminished LV internal dimension at end diastole and LV internal dimension at systole (Figure 2A). The negative control construct shNC-V (the negative control shRNA engineered into the AAV9 vector) failed to affect the ischemia-induced cardiac dysfunction.

The data presented above suggest that upregulation of *ZFAS1* in MI produces deleterious effects on the heart. If this is true, then overexpression of *ZFAS1* in otherwise normal mice should be able to reproduce the phenotypes of MI-induced cardiac contractile dysfunction. To examine this notion, we went on to use the gain-of-function approach for our subsequent experiments using the adeno-associated virus serotype 9 vector carrying the *ZFAS1* gene (*ZFAS1*-V) for its overexpression under in vivo conditions. As depicted in Figure 2B, *ZFAS1*-V, but not the negative control NC-V (the empty AAV9 vector as a negative control for *ZFAS1*-V), significantly reduced EF and fractional shortening and enlarged LV internal dimension at end diastole and LV internal dimension at systole, the effects resembling those induced by MI. These deleterious effects were nearly abolished by sh*ZFAS1*-V to knock down *ZFAS1*, indicating the specificity of actions by *ZFAS1*.

The maximum rate of rise of LV pressure during contraction (+dp/dt$_{max}$) and the maximum rate of drop of LV pressure during relaxation (−dp/dt$_{max}$) have been considered the better manifestations of cardiac contraction and relaxation functions.[39,40] Our results showed marked decreases in ±dp/dt$_{max}$ in MI mice compared with the sham control animals (Figure 2C). Similarly, the healthy mice pretreated with *ZFAS1*-V for overexpression also exhibited substantially reduced ±dp/dt$_{max}$ values relative to control mice. Notably, the decreases in ±dp/dt$_{max}$ induced by *ZFAS1* overexpression were nearly completely reversed by coapplication of sh*ZFAS1*-V (Figure 2C).

The effects of *ZFAS1* on cardiac contractile function revealed by the results described above indicate that *ZFAS1* produces a negative impact on cardiac mechanical function. To test this notion, we compared the contractility of cardiac muscles isolated from MI mice pretreated with sh*ZFAS1*-V or shNC-V and sham-operated control mice. It is well established that sarcomere shortening (SS) is an index of contraction force of cardiac muscles: the longer the SS, the greater the contraction force.[41] This is because an increase in SS can result in shortening of interfilament lattice spacing bringing cross-bridges in closer proximity to actin monomers thereby increasing the number of force generating cross-bridges (Figure 2D, left). We, therefore, used SS to reflect contractility of cardiac muscles. As shown in Figure 2D (middle), SS was pronouncedly shortened in MI mice compared with the sham control animals, indicating the mechanical deficiency under ischemic insults. Strikingly, in the cardiac cells isolated from the MI mice infected with sh*ZFAS1*-V, but not with shNC-V, SS was restored back toward the normal level as that observed in the sham group. Similar to those occurring in MI, in the cardiac fibers isolated from the healthy mice pretreated with *ZFAS1*-V, SS was substantially reduced (Figure 2D, right), whereas SS was unaltered by NC-V. Moreover, the decrease of SS induced by *ZFAS1* overexpression was considerably mitigated by coapplication of sh*ZFAS1*-V.

Successful delivery of sh*ZFAS1*-V and *ZFAS1*-V into the mouse myocardium in vivo was verified by the appreciable presence in myocardial sections of fluorescence signal elicited by GFP (green fluorescent protein) attached to the sh*ZFAS1*-V and *ZFAS1*-V vectors and in mouse myocardium determined by quantitative real-time polymerase chain reaction (Figure 2E; Online Figure IA). Furthermore, the efficiency of sh*ZFAS1*-V to knockdown endogenous *ZFAS1* in MI mice was also confirmed by quantitative real-time polymerase chain reaction showing significant diminishment of

Figure 2 Continued. of fluorescence elicited by GFP (green fluorescent protein) attached to the viral vectors. **F**, Verification of knockdown of endogenous *ZFAS1* by sh*ZFAS1*-V in MI myocardium determined by quantitative real-time-polymerase chain reaction. *P<0.05 vs Sham, #P<0.05 vs MI, §P<0.05 vs sh*ZFAS1*-V; n=≈12–20. **G**, Verification of overexpression of *ZFAS1* elicited by *ZFAS1*-V in normal mice 4 and 7 wk after infection. *P<0.05 vs control, #P<0.05 vs *ZFAS1*-V; n=≈4–10. Data are all expressed as mean±SEM.
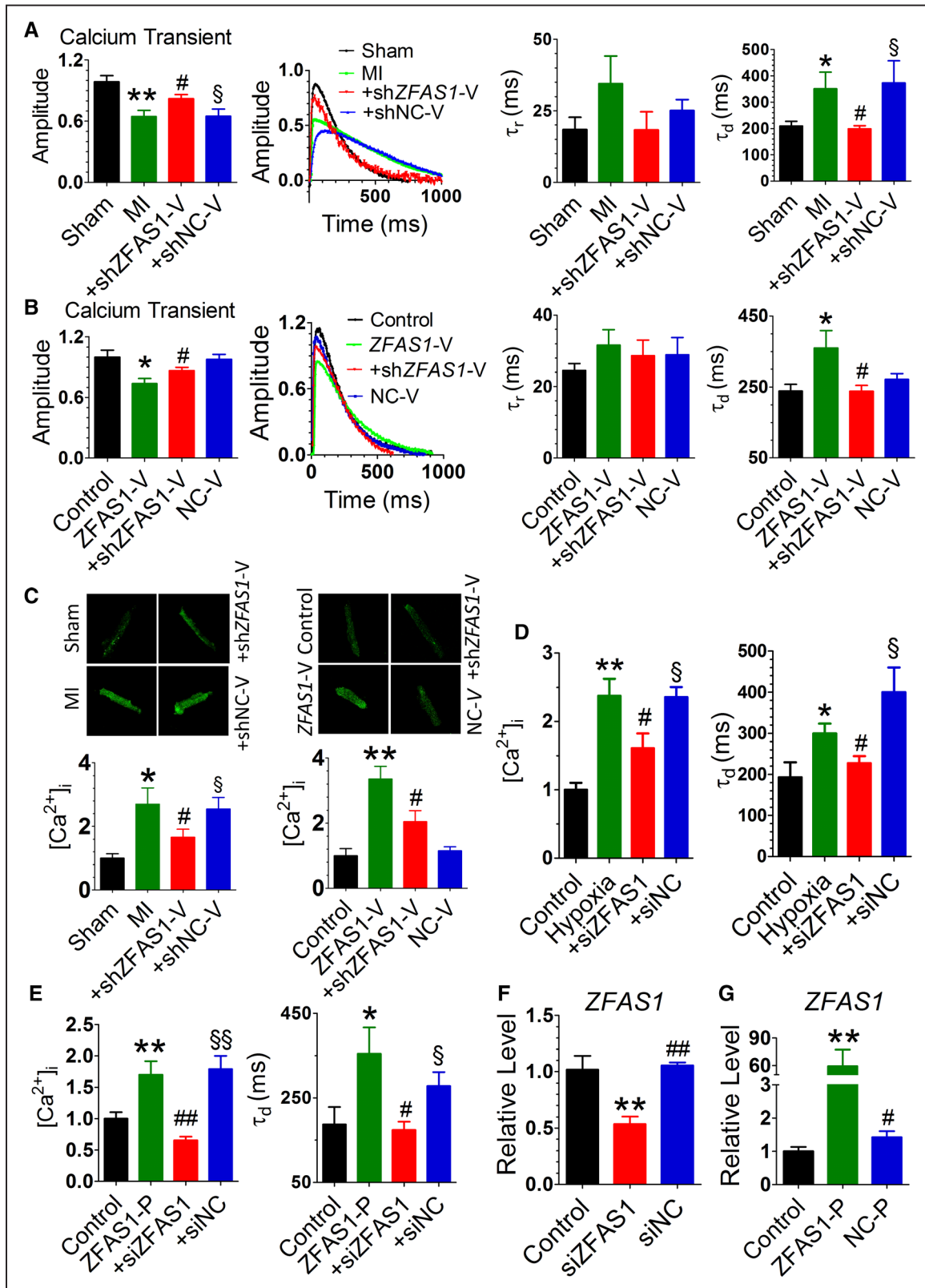
Figure 3. Impairment of intracellular Ca²⁺ homeostasis by *ZFAS1* in cardiomyocytes. A, Restoration of the decreased amplitude of Ca²⁺ transient by adeno-associated virus serotype 9 vector carrying a *ZFAS1*-shRNA fragment (sh*ZFAS1*-V; **left**) and acceleration of the slowed time courses of the rising and decaying phases of Ca²⁺ transient by sh*ZFAS1*-V (**right**) in adult cardiac cells isolated from myocardial infarction (MI) hearts. **P<0.01 vs Sham, #*P*<0.05 vs MI, §*P*<0.05 vs sh*ZFAS1*-V; n=≈17–25. **Middle left**, Typical examples of Ca²⁺ transient traces recorded in Fluo-3-loaded cardiomyocytes isolated from MI mice with or without sh*ZFAS1*-V treatment. **Right**, Averaged data of time constants for sarcoplasmic reticulum (SR) Ca²⁺ release from (τ_r for the rising phase) and Ca²⁺ reuptake back to SR (τ_d for the decaying phase). The time constants were acquired by single exponential curve fitting to the data points (*Continued*)

the *ZFAS1* transcript level in the myocardium (Figure 2F). Overexpression of *ZFAS1* on administration of *ZFAS1*-V for 4 and 7 weeks to healthy mice was also affirmed (Figure 2G; Online Figure IB). As expected, the negative controls NC-V did not affect the *ZFAS1* level, whereas coapplication of sh*ZFAS1*-V and *ZFAS1*-V abolished the overexpression of *ZFAS1*.

Impairment of Intracellular Ca²⁺ Homeostasis by *ZFAS1* in Cardiomyocytes

Ca^{2+} homeostasis is the key determinant of cardiac contractility, and abnormal intracellular Ca^{2+} handling might account at least partially for the observed impairment of contractile function caused by *ZFAS1* in the setting of MI. We, therefore, went on to study the effects of *ZFAS1* on dynamic Ca^{2+} transient and resting intracellular Ca^{2+} concentration ($[Ca^{2+}]_i$), reflecting the intracellular Ca^{2+} handling process and the consequence of alteration of such a process, respectively.[42,43] To this end, the adult ventricular myocytes isolated from MI hearts were loaded with fluo-3 and electrically stimulated at 1 Hz to initiate intracellular Ca^{2+} transients. The amplitude of peak systolic Ca^{2+} transient was calculated according to the equation $(F–F_0)/F_0$, where F represents the maximum value of a Ca^{2+} transient and F_0 the diastolic/resting Ca^{2+} level immediately before the onset of a Ca^{2+} transient, and the time courses of rising (an indication of the rate of SR Ca^{2+} release) and decaying (an indication of the rate of SR Ca^{2+} reuptake) phases were obtained by exponential curve fitting to the raw traces of Ca^{2+} transient. As shown in Figure 3A (left), the amplitude of Ca^{2+} transient was decreased by 34.5% in MI relative to that in sham controls, which was partially but significantly restored toward the normal values in the MI mice pretreated with sh*ZFAS1*-V. More strikingly, the MI-induced prolongation of time course for the decay phase of Ca^{2+} transient was remarkably accelerated by sh*ZFAS1*-V, as reflected by the reduced decay time constant (τ_d; Figure 3A, right). The rate of rising phase of Ca^{2+} transient (τ_r) exhibited a trend of decelerating in MI, and such a slowing was also effectively reversed by knockdown of endogenous *ZFAS1* (Figure 3A, middle right). In all cases, the negative control construct shNC-V did not affect the deleterious alterations in MI mice.

As anticipated, overexpression of *ZFAS1* by *ZFAS1*-V in healthy mice produced the phenotypic changes of Ca^{2+} transient, which were qualitatively the same as those seen in MI mice (Figure 3B). Specifically, *ZFAS1*-V slowed the kinetics

of decaying phases, as the manifested by the remarkable increase of the time constants for Ca^{2+} reuptake (τ_d; Figure 3B, right), and such an effect was completely abrogated by sh*ZFAS1*-V. By comparison, the kinetics of rising phases (τ_r) exhibited a trend to slow, but the alterations did not reach statistical significance (Figure 3B, middle right). Along with the changes of the time constants was a decrease in the amplitude of Ca^{2+} transient with *ZFAS1* overexpression (Figure 3B, left).

The opposite changes of Ca^{2+} transient seen between ischemia or *ZFAS1*-V and sh*ZFAS1*-V predicted a loss of Ca^{2+} homeostasis leading to intracellular Ca^{2+} overload in MI and a relief of such an overload by sh*ZFAS1*-V. The results acquired from the measurements of $[Ca^{2+}]_i$ in adult cardiomyocytes isolated from MI mice and in cultured neonatal cardiomyocytes were indeed in line with this note. As illustrated in Figure 3C (left), the resting $[Ca^{2+}]_i$ in isolated cardiomyocytes from MI mice was increased, and such an increase was abolished by sh*ZFAS1*-V to knockdown endogenous *ZFAS1*. On the contrary, forced expression of *ZFAS1* with *ZFAS1*-V infection directly caused Ca^{2+} overload in healthy mice (Figure 3C, right). These effects of *ZFAS1*-V were effectively reversed by coinjection of sh*ZFAS1*-V, and the negative control NC-V was unable to exert any appreciable impact on $[Ca^{2+}]_i$.

As expected, the resting $[Ca^{2+}]_i$ in NMCMs exposed to hypoxic environment underwent similar changes as in MI: it was increased in hypoxia, and such an increase was abolished by si*ZFAS1* to silence *ZFAS1* expression (Figure 3D, left). Consistent with the increase in $[Ca^{2+}]_i$, the rate of Ca^{2+} reuptake into SR was tremendously slowed (τ_d increased) in hypoxic cells compared with the control group, and this anomaly was essentially rescued by si*ZFAS1* (Figure 3D, right). In sharp contrast to *ZFAS1* silencing, forced expression of *ZFAS1* with transfection of the pCDNA-*ZFAS1* vector directly caused Ca^{2+} overload in nonhypoxic cardiomyocytes (Figure 3E, left). These effects of *ZFAS1* were effectively reversed by cotransfection of si*ZFAS1*, and the negative control construct of si*ZFAS1* was unable to exert any appreciable impact on $[Ca^{2+}]_i$. Expectedly, overexpression of *ZFAS1* was able to induce slowing of τ_d—an effect abrogated by si*ZFAS1*—whereas negative control construct of si*ZFAS1* did not elicit any significant changes (Figure 3E, right).

The effects of sh*ZFAS1*-V and *ZFAS1*-V on Ca^{2+} transient were also assessed by optical mapping techniques. As

Figure 3 Continued. of the rising phase and decaying phase, respectively. *$P<0.05$ vs Sham, #$P<0.05$ vs MI, §$P<0.05$ vs sh*ZFAS1*-V; n=≈15–17. **B**, Decline of the amplitude of Ca^{2+} transient induced by adeno-associated virus 9 vector carrying the *ZFAS1* gene (*ZFAS1*-V; **left**) and increases in the time constants for the rising and decaying phases of Ca^{2+} transient by *ZFAS1*-V (**right**) in adult cardiac cells isolated from healthy mice. **Middle left**, Typical examples of Ca^{2+} transient traces recorded in Fluo-3-loaded cardiomyocytes isolated from healthy mice with or without *ZFAS1*-V or NC-V treatment. **Right**, Mean values of time constants for SR Ca^{2+} release from (τ_r) and Ca^{2+} reuptake (τ_d). *$P<0.05$ vs control or NC-V, #$P<0.05$ vs *ZFAS1*-V; n=≈27–32. **C, Left**, Mitigation of increased intracellular Ca^{2+} concentration ($[Ca^{2+}]_i$) by sh*ZFAS1*-V in MI mice. *$P<0.05$ vs Sham, #$P<0.05$ vs MI, §$P<0.05$ vs sh*ZFAS1*-V; n=≈15–25. **Right**, Elevation of $[Ca^{2+}]_i$ induced by forced expression of *ZFAS1* generated by *ZFAS1*-V infection. **$P<0.01$ vs control and NC-V, #$P<0.05$ vs *ZFAS1*-V; n=≈10–20. **D**, Mitigation of increased intracellular Ca^{2+} concentration ($[Ca^{2+}]_i$) by *ZFAS1* siRNA (si*ZFAS1*; n=≈13–19; **left**) and restoration of the decreased rate of Ca^{2+} reuptake into SR by si*ZFAS1* (n=≈9–13; **right**) in neonatal mouse cardiomyocytes (NMCMs) exposed to hypoxic environment. siRNAs were transfected into cardiomyocytes using X-tremeGENE siRNA transfection reagent. *$P<0.05$, **$P<0.01$ vs control, #$P<0.05$ vs hypoxia, §$P<0.05$ vs si*ZFAS1*. **E, Left**, Elevation of $[Ca^{2+}]_i$ induced by forced expression of *ZFAS1* generated by pCDNA-*ZFAS1* vector (*ZFAS1*-P) in nonhypoxia cardiomyocytes, and abrogation of the effects by cotransfection with si*ZFAS1*. **$P<0.01$ vs control, ##$P<0.01$ vs *ZFAS1*-P, §§$P<0.01$ vs si*ZFAS1*; n=≈11–16. **Right**, Slowing of Ca^{2+} reuptake into SR by forced expression of *ZFAS1* generated by *ZFAS1*-P in nonhypoxia cardiomyocytes, and abrogation of the effects by cotransfection with si*ZFAS1*. *$P<0.05$ vs control, #$P<0.05$ vs *ZFAS1*-P, §$P<0.05$ vs si*ZFAS1*; n=≈8–12. **F**, Verification of the efficacy of si*ZFAS1* to knockdown endogenous *ZFAS1* transcripts in cultured NMCMs. **$P<0.01$ vs control, ##$P<0.01$ vs si*ZFAS1*; n=4. **G**, Verification of overexpression of *ZFAS1* produced by *ZFAS1*-P. **$P<0.01$ vs control, #$P<0.05$ vs *ZFAS1*-P; n=4. siNC indicates scrambled negative control siRNA.
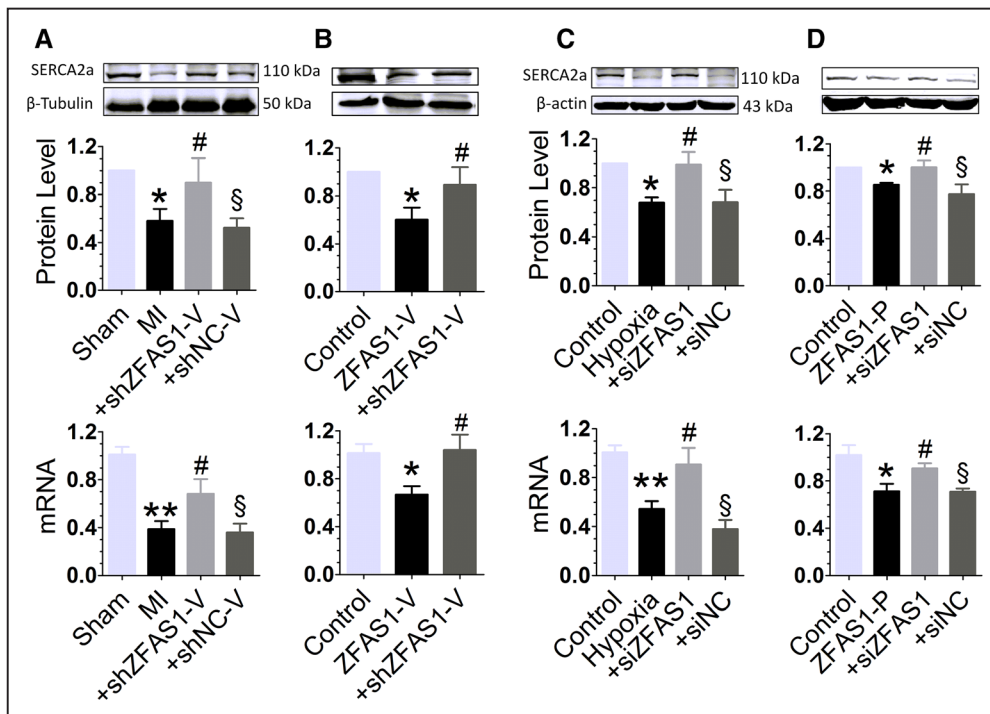
Figure 4. Downregulation of SERCA2a (sarcoplasmic reticulum Ca2+-ATPase 2a) expression induced by *ZFAS1*. A, Downregulation of SERCA2a expression at both protein (**top**) and mRNA (**bottom**) levels in myocardial infarction (MI) hearts relative to the sham animals and recovery of SERCA2a expression by adeno-associated virus serotype 9 vector carrying a *ZFAS1*-shRNA fragment (sh*ZFAS1*-V). *$P<0.05$, **$P<0.01$ vs Sham, #$P<0.05$ vs MI, §$P<0.05$ vs sh*ZFAS1*-V; n=≈6–8. **B**, Downregulation of SERCA2a expression at both protein (**top**) and mRNA (**bottom**) levels in healthy mice pretreated with adeno-associated virus 9 vector carrying the ZFAS1 gene (*ZFAS1*-V) and recovery of SERCA2a expression by sh*ZFAS1*-V. *$P<0.05$ vs control, #$P<0.05$ vs *ZFAS1*-V; n=≈4–6. **C**, Downregulation of SERCA2a expression at both protein (**top**) and mRNA (**bottom**) levels in neonatal mouse cardiomyocytes (NMCMs) cultured under hypoxic conditions relative to the cells in normoxic environment. Note that silence of *ZFAS1* by si*ZFAS1* normalized the SERCA2a expression. *$P<0.05$, **$P<0.01$ vs control, #$P<0.05$ vs hypoxia, §$P<0.05$ vs si*ZFAS1*; n=5. **D**, Downregulation of SERCA2a expression at both protein (**top**) and mRNA (**bottom**) levels by *ZFAS1*-P in NMCMs cultured under normoxic conditions and reversal of SERCA2a downregulation by si*ZFAS1*. *$P<0.05$ vs control, #$P<0.05$ vs *ZFAS1*-P, §$P<0.05$ vs si*ZFAS1*; n=≈4–6. Data are expressed as mean±SEM.

depicted in Online Figure IIA, τ_d was significantly delayed in the heart of MI mice, and this deceleration was countered by sh*ZFAS1*-V. Moreover, overexpression of *ZFAS1* by *ZFAS1*-V was sufficient to reproduce the slowing of Ca²⁺ reuptake in normal mice as that caused by MI (Online Figure IIB).

The efficacy of si*ZFAS1* to knock down endogenous *ZFAS1* in cultured cardiomyocytes was verified by ≈50% reduction of the expression level of *ZFAS1* in si*ZFAS1*-treated cells relative to negative control construct of si*ZFAS1*-treated ones (Figure 3F). Conversely, transfection of pCDNA-*ZFAS1* vector resulted in a robust elevation of *ZFAS1* level, which was not seen with NC-P (the empty pCDNA vector as a negative control for ZFAS1-P; Figure 3G).

Downregulation and Dysfunction of SERCA2a Induced by *ZFAS1*

It has been reported that SERCA2a—the primary cardiac isoform and the key protein involved in sequestration of Ca²⁺ into SR during diastole—plays a major role in the regulation of Ca²⁺ homeostasis in cardiomyocytes.[3] Moreover, SERCA2a has been reported to be abnormally downregulated in a variety of cardiac conditions, including MI.[22,44] The delayed time course of the decaying phase of Ca²⁺ transient by *ZFAS1* in our study suggests an impairment of Ca²⁺ reuptake into SR. A question raised in our mind was whether *ZFAS1* is

involved in the regulation of SERCA2a expression and function or whether alteration of SERCA2a mediates the effects of *ZFAS1*. As shown in Figure 4A, the cardiac expression of SERCA2a at the protein level was prominently decreased in MI mice relative to the sham animals. Similarly, SERCA2a level was also significantly downregulated on overexpression of *ZFAS1* in normal mice (Figure 4B). In both of these situations, sh*ZFAS1*-V rescued the loss of SERCA2a. The expression of SERCA2a mRNA demonstrated qualitatively the same changes as its protein levels (Figure 4A and 4B).

Similar patterns of expression alterations of SERCA2a mRNA and protein were consistently observed in primary NMCMs cultured under hypoxic insult and with treatments with varying constructs (Figure 4C and 4D).

With the above results indicating the significant role of *ZFAS1* in regulating SERCA2a expression, we came up with a further question: Does *ZFAS1* have any direct effects on SERCA2a activities in addition to expression regulation? To get insight into this issue, the first step we took was to perform theoretical analysis for RNA:protein binding using the RNA–Protein Interaction Prediction database. Our analysis revealed a high probability of *ZFAS1*:SERCA2a interaction (Online Figure III). This initial analysis encouraged us to verify the functional relationship between the 2 molecules. We, therefore, switched to an experimental approach using RNA-binding

protein immunoprecipitation to see whether *ZFAS1* could physically bind SERCA2a. The results depicted in Figure 5A clearly indicate the presence of such an interaction: immunoprecipitation of SERCA2a carried an appreciable amount of *ZFAS1*; conversely, RNA pulldown of *ZFAS1* also dragged down an appreciable quantity of SERCA2a (Figure 5B, right), suggesting that *ZFAS1* has a strong affinity to SERCA2a.

If *ZFAS1* indeed binds to SERCA2a, then it should be present in the SR and colocalize with the latter. The purity of SR was verified by the exceptionally enhanced activities of SR-specific NADPH (nicotinamide adenine dinucleotide phosphate) cytochrome C reductase (Figure 5C). The data depicted in Figure 5D show that *ZFAS1* level was significantly increased in the RNA samples isolated from purified SR. Meanwhile, our data exhibited that SERCA2a protein level in SR was significantly decreased (Figure 5E). Moreover, following the same approach described by other groups,[45,46] our immunofluorescent staining of SERCA2a protein in conjunction with GFP-labeling of lncRNA *ZFAS1* demonstrated that *ZFAS1* and SERCA2a proteins had essentially the same subcellular distribution pattern primarily around the nucleus and the 2 molecules colocalized (Online Figure IV).

As already mentioned, in addition to SERCA2a, other proteins, such as RyR2, PLN (phospholamban), and Cav1.2 (the pore-forming α-subunit of L-type Ca^{2+} channels), are also crucially involved in the regulation of intracellular Ca^{2+} homeostasis.[47–49] We, therefore, evaluated the effects of *ZFAS1* on the expression of these proteins. As shown in Online Figure V, no significant alterations of PLN, RyR2, and Cav1.2 protein levels are observed with *ZFAS1* overexpression. Moreover, the lack of effect of *ZFAS1* on L-type Ca^{2+} channel current density further excluded the contribution of this channel to the intracellular Ca^{2+} overload induced by *ZFAS1* (Online Figure VI).

Identification of the Functional Domain of *ZFAS1* Key to the Modulation of SERCA2a

By sequence alignment, we identified a region of high-degree conservation across varying species, including man and mouse (Online Figure VII). We contemplated that this sequence domain might be the functional region for *ZFAS1* (Functional Domain of *ZFAS1* [*ZFAS1*-FD]) to interact with SERCA2a. Our analysis using the computational docking software Hex 8.0[50,51] indeed provided a piece of theoretical evidence for our conjecture by showing the ability of *ZFAS1*-FD to bind SERCA. The docking results obtained by Pymol software revealed that the nucleotides U19, G20, G23, G25, and G26 encompassed by *ZFAS1*-FD are likely the core motif for specific binding to SERCA amino acids Ala^{241}, Glu^{243}, Glu^{689}, Ser^{693}, Arg^{667}, Arg^{671}, and Arg^{672} (Online Figure VIII). Further intriguing was that the SERCA domain that binds *ZFAS1* identified in this study is known to be the phosphorylation domain of SERCA, which contains several potential phosphorylation sites (Ser^{693}, Arg^{667}, and Arg^{671}).[52,53] This information prompted us to further examine our assumption by conducting the following experiments with gain-of-function and loss-of-function approaches.

First, an oligonucleotide fragment corresponding to the conserved region of *ZFAS1* gene (*ZFAS1*-FD; Figure 6A, top) was synthesized. *ZFAS1*-FD was transfected into NMCMs by using X-tremeGENE Transfection Reagent (No. 10810500; Roche) according to the manufacturer's instructions. The ability of *ZFAS1*-FD to bind SERCA2a and its effects on SERCA2a and Ca^{2+} handling were examined. As illustrated in Figure 6B through 6D, application of *ZFAS1*-FD reproduced the effects of full-length *ZFAS1* on SERCA2a expression and intracellular Ca^{2+} status in NMCMs: downregulation of SERCA2a at both protein and mRNA levels (Figure 6B), deceleration of decaying kinetics of Ca^{2+} transient (Figure 6C), and increase in resting Ca^{2+} concentration (Figure 6D). The negative control oligonucleotides fragment (NC) did not produce any of these effects.

Next, we mutated the core motif of the *ZFAS1*-FD by nucleotide substitution to disrupt the binding site for SERCA (Mut-*ZFAS1*-FD; Online Table I) and examined the effects of this construct on SERCA2a function. The computational docking results confirmed the loss of the original binding sites for SERCA in Mut-*ZFAS1*-FD (Online Figure IX). Compared with wild-type *ZFAS1*-FD, Mut-*ZFAS1*-FD failed to affect the expression of SERCA2a at both mRNA and protein levels in NMCMs (Figure 6E), and as anticipated, Mut-*ZFAS1*-FD also lost the ability to alter $[Ca^{2+}]_i$ (Figure 6F) and Ca^{2+} transient (Figure 6G).

We then subsequently constructed an oligonucleotide fragment antisense to *ZFAS1*-FD (As*ZFAS1*-FD; Figure 6A, bottom) with methylation modification to enhance stability. Introduction of As*ZFAS1*-FD into the NMCMs effectively abolished the repressive effect of *ZFAS1* on SERCA2a expression at both mRNA and protein levels, presumably by annealing to *ZFAS1*-FD (Figure 6H). Consistently, As*ZFAS1*-FD also robustly reversed the *ZFAS1*-induced reduction of the amplitude of Ca^{2+} transient (Figure 6I) and delay of the time courses of Ca^{2+} release and reuptake (Figure 6J). By comparison, the negative control antisense fragment failed to affect the effects of *ZFAS1*.

Finally, to verify that the effects of As*ZFAS1*-FD observed in our experiments were indeed attributable to the antisense action, we looked at the changes of *ZFAS1* level in cells treated with the antisense construct. As shown in Figure 6K, the *ZFAS1* level was markedly decreased on transfection with As*ZFAS1*, but not with negative control antisense fragment, in NMCMs pretreated with pCDNA-*ZFAS1* vector.

NFATc2 as a Transactivator of *ZFAS1* Expression

Although the above data have indicated the role of *ZFAS1* upregulation in causing intracellular Ca^{2+} overload and the underlying downstream mechanisms in the setting of MI, it remained unknown how *ZFAS1* was upregulated in MI. To shed light on this issue, we first performed computational analysis and identified several binding sites for NFATc2 (nuclear factor of activated T cells C2) that has been reported to be abundantly expressed in the cardiac tissue and participated in cardiac hypertrophy and heart failure.[54,55] We, therefore, investigated the possible role of NFATc2 in the regulation of *ZFAS1* expression. Our results first demonstrated that the protein level of NFATc2 was robustly upregulated in MI and in NMCMs exposed to hypoxic conditions (Online Figure XA). Application of NFATc2 inhibitor FK506 (10 nmol/L) to NMCMs caused a significant reduction of *ZFAS1* expression relative to nontreated cells
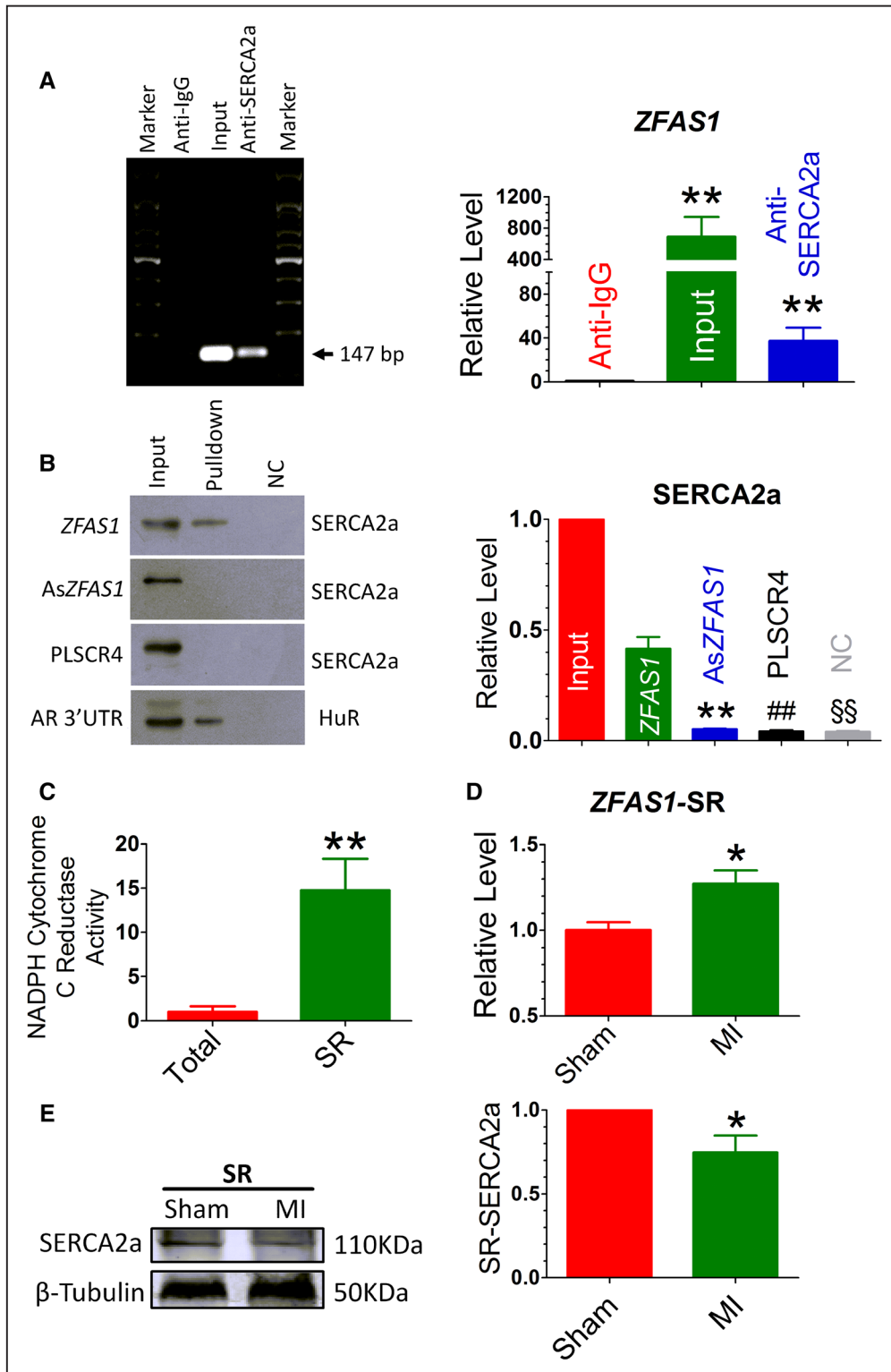
Figure 5. Interaction between lncRNA *ZFAS1* and SERCA2a (sarcoplasmic reticulum Ca^{2+}-ATPase 2a) protein. A, RNA-binding protein immunoprecipitation (RIP) analysis for *ZFAS1*:SERCA2a interaction. Note that immunoprecipitation (IP) of SERCA2a retrieved a robust amount of *ZFAS1*. **$P<0.01$ vs anti-IgG; n=4. **B**, RNA pulldown of *ZFAS1* dragged down an appreciable quantity of SERCA2a. The band for the binding between *ZFAS1* and SERCA2a protein disappeared when treated with an antisense fragment to *ZFAS1* (As*ZFAS1*). Additionally, an unrelated lncRNA PLSCR4 (phospholipid scramblase 4) as a negative control, could not drag down SERCA2a, indicating the specific of the *ZFAS1*:SERCA2a interaction. **$P<0.01$, ##$P<0.01$, §§$P<0.01$ vs *ZFAS1*; n=3. **C**, Verification of the purity of isolated sarcoplasmic reticulum (SR) by the enhanced activity of SR-specific NADPH (nicotinamide adenine dinucleotide phosphate) cytochrome C reductase determined by colorimetry assay. **$P<0.01$ vs total protein samples; n=4. **D**, Upregulation of *ZFAS1* expression in SR isolated from myocardial infarction (MI) hearts relative to Sham hearts, determined by quantitative real-time-polymerase chain reaction. *$P<0.05$ vs Sham; n=3. **E**, Downregulation of SERCA2a protein in SR of MI myocardium relative to sham control, determined by Western blot analysis. *$P<0.05$ vs Sham; n=3.
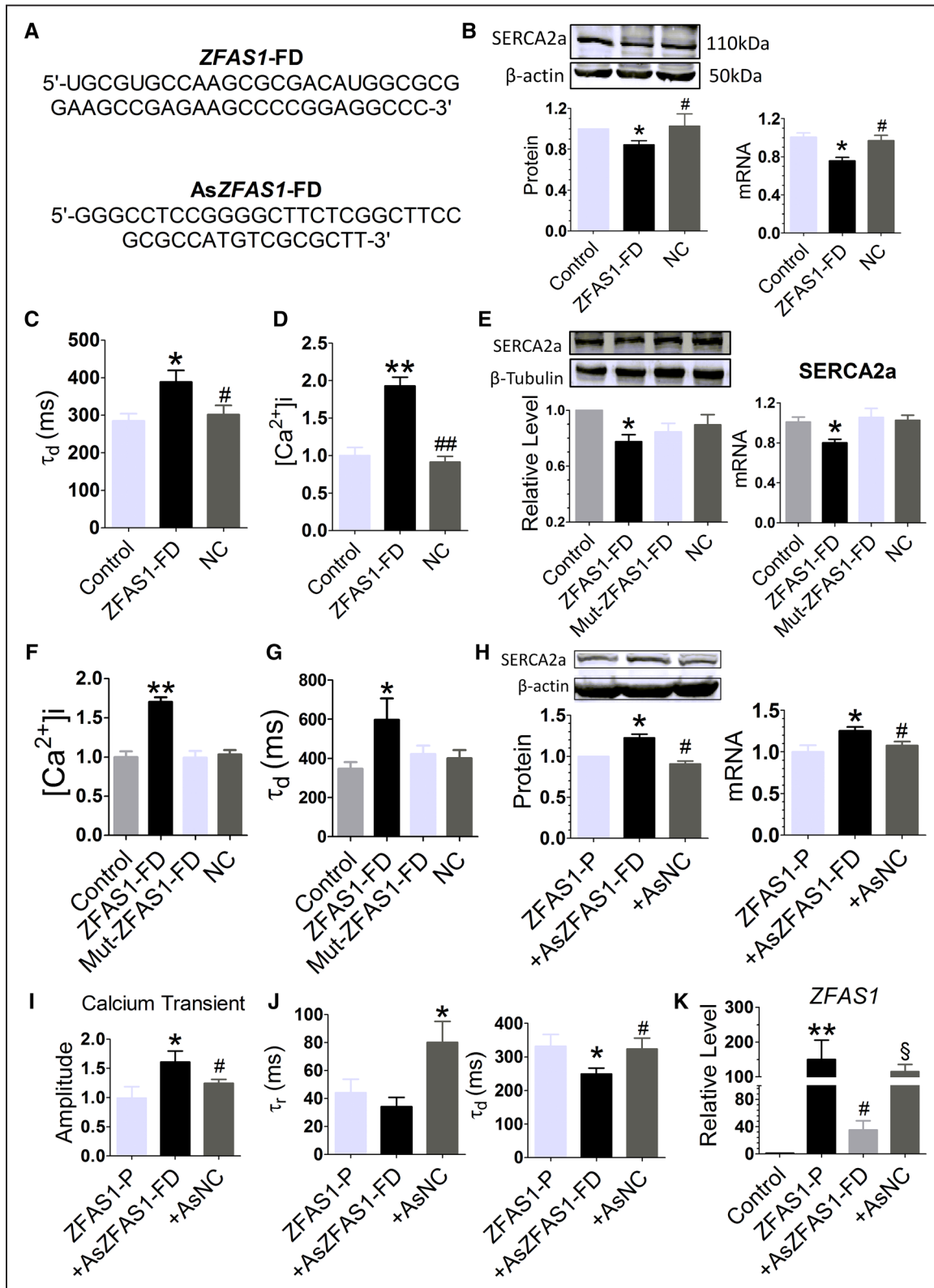
Figure 6. Dysfunction of SERCA2a (sarcoplasmic reticulum Ca²⁺-ATPase 2a) produced by *ZFAS1*. A, Top, An oligonucleotide fragment corresponding to the conserved region of *ZFAS1* gene (functional domain of ZFAS1 [*ZFAS1*-FD]). **Bottom,** An oligonucleotide fragment antisense to *ZFAS1*-FD (As*ZFAS1*-FD). **B,** Downregulation of SERCA2a expression at both protein (**left**) and mRNA (**right**) levels in neonatal mouse cardiomyocytes (NMCMs) transfected with *ZFAS1*-FD. *$P<0.05$ vs control, #$P<0.05$ vs *ZFAS1*-FD; n=≈5–7. **C,** Deceleration of decaying kinetics of Ca²⁺ transient in NMCMs transfected with *ZFAS1*-FD. *$P<0.05$ vs control, #$P<0.05$ vs *ZFAS1*-FD; n=≈17–22. **D,** Increase in resting Ca²⁺ concentration ([Ca²⁺]ᵢ) in NMCMs transfected with *ZFAS1*-FD. **$P<0.01$ vs control, ##$P<0.01$ vs *ZFAS1*-FD; n=≈14–30. **E,** Effects of Mut-*ZFAS1*-FD and *ZFAS1*-FD on the expression of SERCA2a at both protein (**left**) and mRNA (**right**) levels in NMCMs. *$P<0.05$ vs control or NC; n=≈6–8. **F,** Resting Ca²⁺ concentration ([Ca²⁺]ᵢ) in NMCMs transfected (*Continued*)

(Online Figure XB). Moreover, NFATc2 siRNA (siNFATc2) to silence endogenous NFATc2 also downregulated the expression of *ZFAS1*. (Online Figure XC and XD). In addition to NFATc2, NFATc3 (nuclear factor of activated T cells C3)—another NFAT isoform known to be involved in the regulation of Ca^{2+} homeostasis in cardiomyocytes—was also investigated for its possible role in regulation *ZFAS1* expression. Our data exhibited that although NFATc3 expression was also increased in MI and hypoxia, its siRNA did not alter *ZFAS1* expression, consistent with the lack of NFATc3 binding sites in the promoter region of *ZFAS1* gene (Online Figure XE through XG).

Discussion

The aims of this study were to elucidate the pathophysiological role of lncRNA *ZFAS1* and to delineate the underlying mechanisms in the setting of MI. Our data demonstrated that *ZFAS1* was robustly increased in its expression levels in both SR and cytoplasm of MI hearts, and such an upregulation produced significant negative impacts on the heart. This is supported by the finding that knockdown of endogenous *ZFAS1* partially abrogated the ischemia-induced contractile dysfunction. Artificial overexpression of *ZFAS1* in otherwise normal mice created similar impairments of cardiac function as that observed in MI mice. Moreover, at the cellular level, *ZFAS1* overexpression weakened the contractility of cardiac muscles. Furthermore, at the subcellular level, *ZFAS1* deleteriously altered the Ca^{2+} transient leading to intracellular Ca^{2+} overload in cardiomyocytes. At the molecular level, *ZFAS1* was found to directly bind to SERCA2a protein on one hand and to repress its expression on the other hand, the dual actions limiting the activities of this critical Ca^{2+} handling protein. Probably, the most prominent finding is the identification of the *ZFAS1*-FD responsible at least partly for the effects of this lncRNA on SERCA2a and its associated intracellular Ca^{2+} handling process, and the demonstration of As*ZFAS1*-FD was able to mitigate the effects of full-length *ZFAS1*. Finally, evidence was obtained for NFATc2 to account at least partially for the upregulation of *ZFAS1* in MI. These findings allowed us to propose the following paradigm for the regulation of cardiac contractile function by *ZFAS1* in the setting of MI: MI→NFATc2↑→*ZFAS1*↑→SERCA2a↓→$[Ca^{2+}]_i$↑/Ca^{2+} overload→contractility↓→contractile function↓, as schematically illustrated in Online Figure XI. Notably, the effects of *ZFAS1* were found fully reversible on knockdown of this lncRNA. Based on these findings, we concluded that *ZFAS1* is a detrimental lncRNA contributing to cardiac contractile dysfunction through targeting SERCA2a and the associated Ca^{2+} handling in MI.

Comparison With Published Studies on *ZFAS1*

ZFAS1—a new member of lncRNAs—was initially identified in patients with breast tumors and subsequently characterized in other cancers.[56–59] Our recently published study suggested circulating level of *ZFAS1* as a new biomarker for MI because it was found to be considerably decreased of patients with MI.[29] Intriguingly, expression of *ZFAS1* was found to be increased in the myocardium of MI mice—a finding that triggered the present study. During the course of this study, a research article on *ZFAS1* in the heart was published.[60] In agreement with our finding with MI mice, the authors showed that *ZFAS1* is upregulated in a rat model of acute MI, and such an increase induces cardiomyocyte apoptosis. They further demonstrated that *ZFAS1* promotes apoptosis by acting as a ceRNA to reduce the functional availability of miR-150 to increase the level of C-reactive protein.[60] The finding in the present study that *ZFAS1* caused intracellular Ca^{2+} overload might be an alternative mechanism for its proapoptotic property. Yet, future studies are required to verify this point.

Here, we presented the experimental data with both an animal model of MI and a cellular model of hypoxia clearly indicating the pathophysiological function of *ZFAS1* in the regulation of cardiac contractile function. Specifically, abnormal upregulation of *ZFAS1* in MI or artificial overexpression of *ZFAS1* weakened the contractility of cardiac muscles. It seems that the detrimental action of *ZFAS1* on contractility is likely accounted for by impaired intracellular Ca^{2+} handling process. *ZFAS1* produced a negative effect on SERCA2a—a key protein in the homeostasis of intracellular Ca^{2+}—via dual mechanisms: expression repression of SERCA2a gene and functional restriction of SERCA2a protein. Reduced SERCA2a availability resulted in a decrease in Ca^{2+} reuptake back into SR leading to intracellular Ca^{2+} overload, the latter of which is likely the main detrimental factor for cardiac dysfunction. Our study ruled out the significant contribution of other Ca^{2+} handling-regulatory proteins, such as RyR2, PLN, and L-type Ca^{2+} channels to *ZFAS1*-induced deleterious alterations. These results in conjunction with those reported by Wu et al[60] suggest that *ZFAS1* affects cardiac function through at least 2 different processes or pathways: intracellular Ca^{2+} overload and apoptotic cell death.

An interesting finding in the present study is that the sequence domain of the *ZFAS1* gene that is conserved across species mimicked the effects of the full-length *ZFAS1* in terms of its effects on SERCA2a expression and functionality and on the associated slowing of decaying process of Ca^{2+} transient and increase in resting Ca^{2+} concentration. More strikingly, mutation of this domain rendered a loss of its ability to regulate SERCA2a and $[Ca^{2+}]_i$, and an antisense fragment to the conserved region of *ZFAS1* gene efficiently canceled out the deleterious actions of *ZFAS1*. The computational docking analysis further unraveled the potential direct interaction between *ZFAS1*-FD and SERCA2a. Such analysis also revealed

Figure 6 Continued. with Mut-*ZFAS1*-FD. **P<0.01 vs control or NC; n=≈25–36. **G**, The decaying kinetics of Ca^{2+} transient in NMCMs transfected with Mut-*ZFAS1*-FD. *P<0.05 vs control or NC; n=≈9–12. **H**, Upregulation of SERCA2a expression at both protein (**left**) and mRNA (**right**) levels by As*ZFAS1*-FD in NMCMs pretreated with *ZFAS1*-P for *ZFAS1* overexpression. *P<0.05 vs *ZFAS1*-P, #*P*<0.05 vs As*ZFAS1*-FD; n=≈5–9. **I**, Reversal of *ZFAS1*-induced reduction of Ca^{2+} transient amplitude by As*ZFAS1*-FD. *P<0.05 vs *ZFAS1*-P, #*P*<0.05 vs As*ZFAS1*-FD; n=≈10–18. **J**, Reversal of the time delay of Ca^{2+} release and reuptake by As*ZFAS1*-FD in NMCMs pretreated with *ZFAS1*-P for *ZFAS1* overexpression. *P<0.05 vs As*ZFAS1*-FD (**left**) or *ZFAS1*-P (**right**), #*P*<0.05 vs As*ZFAS1*-FD; n=≈12–18. **K**, Verification of the efficacy of As*ZFAS1*-FD in reducing *ZFAS1* level in NMCMs pretreated with *ZFAS1*-P for *ZFAS1* overexpression. **P<0.01 vs control, #*P*<0.05 vs *ZFAS1*-P, §*P*<0.05 vs As*ZFAS1*-FD; n=6.

the core motif with specific nucleotides contained in *ZFAS1*-FD being responsible for binding to a SERCA domain containing amino acids Ala[241], Glu[243], Glu[689], Ser[693], Arg[667], Arg[671], and Arg[672]. Most strikingly, the SERCA domain that binds *ZFAS1* identified in this study is right within the phosphorylation domain of SERCA, which contains several potential phosphorylation sites (Ser[693], Arg[667], and Arg[671]).[52,53] It is known that SERCA pumps are P-type ion motive ATPases that in their sequence structures contain 3 major domains on the cytoplasmic face: the phosphorylation domain (or phosphorylation domain), nucleotide-binding domain, and the actuator domain.[52,53] Although PLN phosphorylation to increase the affinity of SERCA2 for Ca^{2+} is the most important modulation of this protein, direct CaMKII (calmodulin-dependent protein kinase II)-dependent phosphorylation of SERCA2 has also been documented to be an important route to control the enzyme function,[61,62] particularly when considering the fact that PLN was unaffected by *ZFAS1* in our models. Direct phosphorylation at residue Ser[38] in SERCA2a activates enzyme function and enhances Ca^{2+} reuptake into SR and cardiac contractility.[63] It is possible that SERCA2a can also be activated with its phosphorylation domain being phosphorylated, and when bounded by *ZFAS1*, the phosphorylation sites of phosphorylation domain are masked by the latter. Such masking would prevent SERCA2a from being phosphorylated by CaMKII or other kinases thereby preventing SERCA2a from being activated. At present, such a view is highly speculative and requires rigorous studies to clarify. Nonetheless, these facts together with our findings would suggest that we have identified the *ZFAS1*-FD responsible for the effects of this lncRNA on SERCA2a and its associated intracellular Ca^{2+} handling process.

Potential Implications of Our Findings

The findings in the present study, together with the published studies from our own laboratory[29] and from other research group,[60] indicate that *ZFAS1* is not only a biomarker for, or predictor of, MI but also a determinant of cardiac function in the setting of MI and might be in other cardiovascular pathological processes as well. In particular, the fact that knockdown of *ZFAS1* is able to rescue the deleterious actions of *ZFAS1* on cardiac function opens up an opportunity for correcting the functional impairment of heart caused by ischemia/hypoxia. This would imply that *ZFAS1* could be considered a novel therapeutic target for maintaining cardiac function in MI. Or in other words, sh*ZFAS1*-V or other forms of *ZFAS1* inhibitor could be developed into novel therapeutic agent for ameliorating cardiac dysfunction.

In addition, our finding that As*ZFAS1*-FD was also able to eliminate the detrimental action of *ZFAS1* on SERCA2a and cardiac function suggests that antisense is another valid strategy for the management of MI-induced cardiac impairment. Such an antisense strategy might be even superior to the knockdown approach because it targets directly to the functional domain of the lncRNA, and it does not induce breakdown of *ZFAS1* but merely reduces the functional availability of it. One of the advantages of these properties is that on withdraw of the antisense, the function of *ZFAS1* could readily recover.

Possible Limitations of Our Study

We are well aware that our study contains several limitations. First, despite that *ZFAS1* elicited remarkable suppressive effects on SERCA2a and the associated Ca^{2+} transient decaying kinetics and contractility, it did not cause proportional depression of cardiac function (EF and fractional shortening). One possible explanation for this is that *ZFAS1* might also be able to evoke some other actions in addition to SERCA2a inhibition, which could relieve its detrimental effects and partially preserve the cardiac function. Second, although we have identified a sequence motif that is evidently important to the role of *ZFAS1* in regulating SERCA2a and is reasonably well conserved between mouse and human, the conclusion drawn from our animal study may not be extrapolated directly to man. And third, the present study does not answer the question how *ZFAS1* altered the mRNA level of SERCA2a. There are a couple of possible explanations for the observation. First, *ZFAS1* might act as transcriptional repressor by modifying the chromatin structure/methylation or indirectly by regulating relevant transcriptional factors or RNA maturation via epigenetic modifications. In addition, lncRNAs can also interact with mRNAs through direct antisense binding to either stabilize or induce degradation of the targeted mRNAs. We found that *ZFAS1* carries several sequence stretches that are complementary to the 3′-end untranslated region of SERCA2a, and such an antisense relationship might impose a direct interaction between *ZFAS1* and SERCA2a mRNA to alter the expression levels mutually. Yet, rigorous future studies are required to clarify these issues.

Disclosures

None.

References

1. Luo M, Anderson ME. Mechanisms of altered Ca^{2+} handling in heart failure. *Circ Res*. 2013;113:690–708. doi: 10.1161/CIRCRESAHA.113.301651.
2. Li XC, Wei L, Zhang GQ, Bai ZL, Hu YY, Zhou P, Bai SH, Chai Z, Lakatta EG, Hao XM, Wang SQ. Ca2+ cycling in heart cells from ground squirrels: adaptive strategies for intracellular Ca^{2+} homeostasis. *PLoS One*. 2011;6:e24787. doi: 10.1371/journal.pone.0024787.
3. Park WJ, Oh JG. SERCA2a: a prime target for modulation of cardiac contractility during heart failure. *BMB Rep*. 2013;46:237–243.
4. Xin W, Lu X, Li X, Niu K, Cai J. Attenuation of endoplasmic reticulum stress-related myocardial apoptosis by SERCA2a gene delivery in ischemic heart disease. *Mol Med*. 2011;17:201–210. doi: 10.2119/molmed.2010.00197.
5. Younce CW, Burmeister MA, Ayala JE. Exendin-4 attenuates high glucose-induced cardiomyocyte apoptosis via inhibition of endoplasmic reticulum stress and activation of SERCA2a. *Am J Physiol Cell Physiol*. 2013;304:C508–C518. doi: 10.1152/ajpcell.00248.2012.
6. Kawase Y, Hajjar RJ. The cardiac sarcoplasmic/endoplasmic reticulum calcium ATPase: a potent target for cardiovascular diseases. *Nat Clin Pract Cardiovasc Med*. 2008;5:554–565. doi: 10.1038/ncpcardio1301.
7. Faria Tde O, Costa GP, Almenara CC, Angeli JK, Vassallo DV, Stefanon I, Vassallo PF. Chronic exposure to low doses of HgCl2 avoids calcium handling impairment in the right ventricle after myocardial infarction in rats. *PLoS One*. 2014;9:e95639. doi: 10.1371/journal.pone.0095639.

8. Kawase Y, Ly HQ, Prunier F, et al. Reversal of cardiac dysfunction after long-term expression of SERCA2a by gene transfer in a pre-clinical model of heart failure. *J Am Coll Cardiol*. 2008;51:1112–1119. doi: 10.1016/j.jacc.2007.12.014.

9. Lipskaia L, Hadri L, Lopez JJ, Hajjar RJ, Bobe R. Benefit of SERCA2a gene transfer to vascular endothelial and smooth muscle cells: a new aspect in therapy of cardiovascular diseases. *Curr Vasc Pharmacol*. 2013;11:465–479.

10. Sun X, Zhong J, Wang D, Xu J, Su H, An C, Zhu H, Yan J. Increasing glutamate promotes ischemia-reperfusion-induced ventricular arrhythmias in rats in vivo. *Pharmacology*. 2014;93:4–9. doi: 10.1159/000356311.

11. Zsebo K, Yaroshinsky A, Rudy JJ, Wagner K, Greenberg B, Jessup M, Hajjar RJ. Long-term effects of AAV1/SERCA2a gene transfer in patients with severe heart failure: analysis of recurrent cardiovascular events and mortality. *Circ Res*. 2014;114:101–108. doi: 10.1161/CIRCRESAHA. 113.302421.

12. Kho C, Lee A, Jeong D, Oh JG, Gorski PA, Fish K, Sanchez R, DeVita RJ, Christensen G, Dahl R, Hajjar RJ. Small-molecule activation of SERCA2a SUMOylation for the treatment of heart failure. *Nat Commun*. 2015;6:7229. doi: 10.1038/ncomms8229.

13. Sikkel MB, Hayward C, MacLeod KT, Harding SE, Lyon AR. SERCA2a gene therapy in heart failure: an anti-arrhythmic positive inotrope. *Br J Pharmacol*. 2014;171:38–54. doi: 10.1111/bph.12472.

14. Greenberg B, Butler J, Felker GM, Ponikowski P, Voors AA, Desai AS, Barnard D, Bouchard A, Jaski B, Lyon AR, Pogoda JM, Rudy JJ, Zsebo KM. Calcium upregulation by percutaneous administration of gene therapy in patients with cardiac disease (CUPID 2): a randomised, multinational, double-blind, placebo-controlled, phase 2b trial. *Lancet*. 2016;387:1178–1186. doi: 10.1016/S0140-6736(16)00082-9.

15. Mehta LS, Beckie TM, DeVon HA, Grines CL, Krumholz HM, Johnson MN, Lindley KJ, Vaccarino V, Wang TY, Watson KE, Wenger NK; American Heart Association Cardiovascular Disease in Women and Special Populations Committee of the Council on Clinical Cardiology; Council on Epidemiology and Prevention; Council on Cardiovascular and Stroke Nursing; Council on Quality of Care and Outcomes Research. Acute myocardial infarction in women: a scientific statement from the American Heart Association. *Circulation*. 2016;133:916–947. doi: 10.1161/CIR.0000000000000351.

16. Saxena A, Russo I, Frangogiannis NG. Inflammation as a therapeutic target in myocardial infarction: learning from past failures to meet future challenges. *Transl Res*. 2016;167:152–166. doi: 10.1016/j.trsl.2015.07.002.

17. Muthuramu I, Lox M, Jacobs F, De Geest B. Permanent ligation of the left anterior descending coronary artery in mice: a model of post-myocardial infarction remodelling and heart failure. *J Vis Exp*. 2014;94:e52206. doi: 10.3791/52206.

18. Cabello JB, Burls A, Emparanza JI, Bayliss SE, Quinn T. Oxygen therapy for acute myocardial infarction. *Cochrane Database Syst Rev*. 2016;12:CD007160. doi: 10.1002/14651858.CD007160.pub4.

19. Webster KA. Mitochondrial membrane permeabilization and cell death during myocardial infarction: roles of calcium and reactive oxygen species. *Future Cardiol*. 2012;8:863–884. doi: 10.2217/fca.12.58.

20. Kemi OJ, MacQuaide N, Hoydal MA, Ellingsen O, Smith GL, Wisloff U. Exercise training corrects control of spontaneous calcium waves in hearts from myocardial infarction heart failure rats. *J Cell Physiol*. 2012;227:20–26. doi: 10.1002/jcp.22771.

21. Murakoshi M, Saiki K, Urayama K, Sato TN. An anthelmintic drug, pyrvinium pamoate, thwarts fibrosis and ameliorates myocardial contractile dysfunction in a mouse model of myocardial infarction. *PLoS One*. 2013;8:e79374. doi: 10.1371/journal.pone.0079374.

22. Melo SF, Barauna VG, Neves VJ, Fernandes T, Lara Lda S, Mazzotti DR, Oliveira EM. Exercise training restores the cardiac microRNA-1 and -214 levels regulating Ca2+ handling after myocardial infarction. *BMC Cardiovasc Disord*. 2015;15:166. doi: 10.1186/s12872-015-0156-4.

23. Talukder MA, Kalyanasundaram A, Zhao X, Zuo L, Bhupathy P, Babu GJ, Cardounel AJ, Periasamy M, Zweier JL. Expression of SERCA isoform with faster Ca2+ transport properties improves postischemic cardiac function and Ca2+ handling and decreases myocardial infarction. *Am J Physiol Heart Circ Physiol*. 2007;293:H2418–H2428. doi: 10.1152/ajpheart.00663.2007.

24. Fernandes AA, Ribeiro RF Jr, de Moura VG, Siman FD, Dias FM, Zoghaib J, Vassallo PF, Vassallo DV, Stefanon I. SERCA-2a is involved in the right ventricular function following myocardial infarction in rats. *Life Sci*. 2015;124:24–30. doi: 10.1016/j.lfs.2015.01.010.

25. Derrien T, Johnson R, Bussotti G, et al. The GENCODE v7 catalog of human long noncoding RNAs: analysis of their gene structure, evolution, and expression. *Genome Res*. 2012;22:1775–1789. doi: 10.1101/gr.132159.111.

26. Djebali S, Davis CA, Merkel A, et al. Landscape of transcription in human cells. *Nature*. 2012;489:101–108. doi: 10.1038/nature11233.

27. Kumarswamy R, Bauters C, Volkmann I, Maury F, Fetisch J, Holzmann A, Lemesle G, de Groote P, Pinet F, Thum T. Circulating long noncoding RNA, LIPCAR, predicts survival in patients with heart failure. *Circ Res*. 2014;114:1569–1575. doi: 10.1161/CIRCRESAHA.114.303915.

28. Wang K, Liu CY, Zhou LY, Wang JX, Wang M, Zhao B, Zhao WK, Xu SJ, Fan LH, Zhang XJ, Feng C, Wang CQ, Zhao YF, Li PF. APF lncRNA regulates autophagy and myocardial infarction by targeting miR-188-3p. *Nat Commun*. 2015;6:6779. doi: 10.1038/ncomms7779.

29. Zhang Y, Sun L, Xuan L, et al. Reciprocal changes of circulating long noncoding RNAs ZFAS1 and CDR1AS predict acute myocardial infarction. *Sci Rep*. 2016;6:22384. doi: 10.1038/srep22384.

30. Wang K, Liu F, Zhou LY, Long B, Yuan SM, Wang Y, Liu CY, Sun T, Zhang XJ, Li PF. The long noncoding RNA CHRF regulates cardiac hypertrophy by targeting miR-489. *Circ Res*. 2014;114:1377–1388. doi: 10.1161/CIRCRESAHA.114.302476.

31. Wang K, Long B, Zhou LY, Liu F, Zhou QY, Liu CY, Fan YY, Li PF. CARL lncRNA inhibits anoxia-induced mitochondrial fission and apoptosis in cardiomyocytes by impairing miR-539-dependent PHB2 downregulation. *Nat Commun*. 2014;5:3596. doi: 10.1038/ncomms4596.

32. Zhang X, Sha M, Yao Y, Da J, Jing D. Increased B-type-natriuretic peptide promotes myocardial cell apoptosis via the B-type-natriuretic peptide/long non-coding RNA LSINCT5/caspase-1/interleukin 1β signaling pathway. *Mol Med Rep*. 2015;12:6761–6767. doi: 10.3892/mmr.2015.4247.

33. Han P, Li W, Lin CH, et al. A long noncoding RNA protects the heart from pathological hypertrophy. *Nature*. 2014;514:102–106. doi: 10.1038/nature13596.

34. Liu L, An X, Li Z, Song Y, Li L, Zuo S, Liu N, Yang G, Wang H, Cheng X, Zhang Y, Yang X, Wang J. The H19 long noncoding RNA is a novel negative regulator of cardiomyocyte hypertrophy. *Cardiovasc Res*. 2016;111:56–65. doi: 10.1093/cvr/cvw078.

35. Xuan L, Sun L, Zhang Y, et al. Circulating long non-coding RNAs NRON and MHRT as novel predictive biomarkers of heart failure. *J Cell Mol Med*. 2017;21:1803–1814. doi: 10.1111/jcmm.13101.

36. Aurora AB, Mahmoud AI, Luo X, Johnson BA, van Rooij E, Matsuzaki S, Humphries KM, Hill JA, Bassel-Duby R, Sadek HA, Olson EN. MicroRNA-214 protects the mouse heart from ischemic injury by controlling Ca2+ overload and cell death. *J Clin Invest*. 2012;122:1222–1232. doi: 10.1172/JCI59327.

37. Regula KM, Ens K, Kirshenbaum LA. Inducible expression of BNIP3 provokes mitochondrial defects and hypoxia-mediated cell death of ventricular myocytes. *Circ Res*. 2002;91:226–231.

38. Inagaki K, Fuess S, Storm TA, Gibson GA, Mctiernan CF, Kay MA, Nakai H. Robust systemic transduction with AAV9 vectors in mice: efficient global cardiac gene transfer superior to that of AAV8. *Mol Ther*. 2006;14:45–53. doi: 10.1016/j.ymthe.2006.03.014.

39. Parekh R, Kolias TJ. A novel noninvasive method to assess left ventricular -dP/dt using diastolic blood pressure and isovolumic relaxation time. *Echocardiography*. 2013;30:267–270. doi: 10.1111/echo.12042.

40. Buchanan LV, Warner WA, Arthur SR, Gleason CR, Lewen G, Levesque PC, Gill MW. Evaluation of cardiac function in unrestrained dogs and monkeys using left ventricular dP/dt. *J Pharmacol Toxicol Methods*. 2016;80:51–58. doi: 10.1016/j.vascn.2016.03.006.

41. Hobai IA, Morse JC, Siwik DA, Colucci WS. Lipopolysaccharide and cytokines inhibit rat cardiomyocyte contractility in vitro. *J Surg Res*. 2015;193:888–901. doi: 10.1016/j.jss.2014.09.015.

42. Kobayashi S, Susa T, Ishiguchi H, et al. A low-dose β1-blocker in combination with milrinone improves intracellular Ca2+ handling in failing cardiomyocytes by inhibition of milrinone-induced diastolic Ca2+ leakage from the sarcoplasmic reticulum. *PLoS One*. 2015;10:e0114314. doi: 10.1371/journal.pone.0114314.

43. Gómez-Viquez NL, Guerrero-Serna G, Arvizu F, García U, Guerrero-Hernández A. Inhibition of SERCA pumps induces desynchronized RyR activation in overloaded internal Ca2+ stores in smooth muscle cells. *Am J Physiol Cell Physiol*. 2010;298:C1038–C1046. doi: 10.1152/ajpcell.00222.2009.

44. Zalvidea S, André L, Loyer X, Cassan C, Sainte-Marie Y, Thireau J, Sjaastad I, Heymes C, Pasquié JL, Cazorla O, Aimond F, Richard S. ACE inhibition prevents diastolic Ca2+ overload and loss of myofilament Ca2+ sensitivity after myocardial infarction. *Curr Mol Med*. 2012;12:206–217.

45. Nelson BR, Makarewich CA, Anderson DM, Winders BR, Troupes CD, Wu F, Reese AL, McAnally JR, Chen X, Kavalali ET, Cannon SC, Houser

SR, Bassel-Duby R, Olson EN. A peptide encoded by a transcript annotated as long noncoding RNA enhances SERCA activity in muscle. *Science*. 2016;351:271–275. doi: 10.1126/science.aad4076.

46. Anderson DM, Anderson KM, Chang CL, Makarewich CA, Nelson BR, McAnally JR, Kasaragod P, Shelton JM, Liou J, Bassel-Duby R, Olson EN. A micropeptide encoded by a putative long noncoding RNA regulates muscle performance. *Cell*. 2015;160:595–606. doi: 10.1016/j.cell.2015.01.009.

47. Zhao G, Li T, Brochet DX, Rosenberg PB, Lederer WJ. STIM1 enhances SR Ca2+ content through binding phospholamban in rat ventricular myocytes. *Proc Natl Acad Sci USA*. 2015;112:E4792–E4801. doi: 10.1073/pnas.1423295112.

48. Yang Y, Guo T, Oda T, Chakraborty A, Chen L, Uchinoumi H, Knowlton AA, Fruen BR, Cornea RL, Meissner G, Bers DM. Cardiac myocyte Z-line calmodulin is mainly RyR2-bound, and reduction is arrhythmogenic and occurs in heart failure. *Circ Res*. 2014;114:295–306. doi: 10.1161/CIRCRESAHA.114.302857.

49. Weiss S, Oz S, Benmocha A, Dascal N. Regulation of cardiac L-type Ca2+ channel CaV1.2 via the β-adrenergic-cAMP-protein kinase A pathway: old dogmas, advances, and new uncertainties. *Circ Res*. 2013;113:617–631. doi: 10.1161/CIRCRESAHA.113.301781.

50. Rahim AH, Setiawan B, Dewi FR, Noor Z. Regulation by phloroglucinol of Nrf2/Maf-mediated expression of antioxidant enzymes and inhibition of osteoclastogenesis via the RANKL/RANK signaling pathway: in silico study. *Acta Inform Med*. 2015;23:228–232. doi: 10.5455/aim.2015.23.228-232.

51. Raharjo SJ, Kikuchi T. Molecular dynamic screening sesquiterpenoid pogostemon herba as suggested cyclooxygenase inhibitor. *Acta Inform Med*. 2016;24:332–337. doi: 10.5455/aim.2016.24.332-337.

52. Sørensen TL, Møller JV, Nissen P. Phosphoryl transfer and calcium ion occlusion in the calcium pump. *Science*. 2004;304:1672–1675. doi: 10.1126/science.1099366.

53. Zhang P, Toyoshima C, Yonekura K, Green NM, Stokes DL. Structure of the calcium pump from sarcoplasmic reticulum at 8-A resolution. *Nature*. 1998;392:835–839. doi: 10.1038/33959.

54. Bourajjaj M, Armand AS, da Costa Martins PA, Weijts B, van der Nagel R, Heeneman S, Wehrens XH, De Windt LJ. NFATc2 is a necessary mediator of calcineurin-dependent cardiac hypertrophy and heart failure. *J Biol Chem*. 2008;283:22295–22303. doi: 10.1074/jbc.M801296200.

55. Chaudhry A, Carthan KA, Kang BY, Calvert J, Sutliff RL, Michael Hart C. PPARγ attenuates hypoxia-induced hypertrophic transcriptional pathways in the heart. *Pulm Circ*. 2017;7:98–107. doi: 10.1086/689749.

56. Askarian-Amiri ME, Crawford J, French JD, Smart CE, Smith MA, Clark MB, Ru K, Mercer TR, Thompson ER, Lakhani SR, Vargas AC, Campbell IG, Brown MA, Dinger ME, Mattick JS. SNORD-host RNA Zfas1 is a regulator of mammary development and a potential marker for breast cancer. *RNA*. 2011;17:878–891. doi: 10.1261/rna.2528811.

57. Nie F, Yu X, Huang M, Wang Y, Xie M, Ma H, Wang Z, De W, Sun M. Long noncoding RNA ZFAS1 promotes gastric cancer cells proliferation by epigenetically repressing KLF2 and NKD2 expression. *Oncotarget*. 2017;8:38227–38238. doi: 10.18632/oncotarget.9611.

58. Thorenoor N, Faltejskova-Vychytilova P, Hombach S, Mlcochova J, Kretz M, Svoboda M, Slaby O. Long non-coding RNA ZFAS1 interacts with CDK1 and is involved in p53-dependent cell cycle control and apoptosis in colorectal cancer. *Oncotarget*. 2016;7:622–637. doi: 10.18632/oncotarget.5807.

59. Xia B, Hou Y, Chen H, Yang S, Liu T, Lin M, Lou G. Long non-coding RNA ZFAS1 interacts with miR-150-5p to regulate Sp1 expression and ovarian cancer cell malignancy. *Oncotarget*. 2017;8:19534–19546. doi: 10.18632/oncotarget.14663.

60. Wu T, Wu D, Wu Q, Zou B, Huang X, Cheng X, Wu Y, Hong K, Li P, Yang R, Li Y, Cheng Y. Knockdown of long non-coding RNA-ZFAS1 protects cardiomyocytes against acute myocardial infarction via anti-apoptosis by regulating miR-150/CRP. *J Cell Biochem*. 2017;118:3281–3289. doi: 10.1002/jcb.25979.

61. Vangheluwe P, Raeymaekers L, Dode L, Wuytack F. Modulating sarco(endo)plasmic reticulum Ca2+ ATPase 2 (SERCA2) activity: cell biological implications. *Cell Calcium*. 2005;38:291–302. doi: 10.1016/j.ceca.2005.06.033.

62. Xu A, Narayanan N. Ca2+/calmodulin-dependent phosphorylation of the Ca2+-ATPase, uncoupled from phospholamban, stimulates Ca2+-pumping in native cardiac sarcoplasmic reticulum. *Biochem Biophys Res Commun*. 1999;258:66–72. doi: 10.1006/bbrc.1999.0579.

63. Toyofuku T, Curotto Kurzydlowski K, Narayanan N, MacLennan DH. Identification of Ser38 as the site in cardiac sarcoplasmic reticulum Ca(2+)-ATPase that is phosphorylated by Ca2+/calmodulin-dependent protein kinase. *J Biol Chem*. 1994;269:26492–26496.